Spring 5-7-2022

Application of the Formal Design of Experiments to Deformed Airfoil Testing

Alex Ligman

Application of the Formal Design of Experiments to Deformed Airfoil Testing

by
Alexander Ligman

A thesis submitted to the faculty of The University of Mississippi in partial fulfillment of the requirements of the Sally McDonnell Barksdale Honors College.

Oxford
May 2022

Approved by

_____
Advisor: Dr. Nathan Murray

_____
Reader: Dr. Sasan Nouranian

_____
Reader: Stephen Perry

Dedication

I dedicate this thesis to my family and friends, without the support of, nothing I do would be possible.

Acknowledgements

My sincere appreciation goes to many people that, without, I would not have been able to accomplish this thesis. Firstly, my thanks goes to Dr. Murray, who graciously allowed me to work under him on this project and gave me this exciting opportunity; further, in helping me understand and appreciate the effort that goes into the scientific method, and experimentation; as well, to Dr. Adam Green who, without his tenacious efforts in fixing the wind tunnel, the experiment could not have been performed; also, to Stephen Perry, who patiently listened to my many questions and was always willing to lend a helping hand, even if he was tired, and who helped me at every stage of the project; to Dr. Nouranian, who gave me advice and guidance on the design of experiments; to Kevin Kwas, who was readily willing to manufacture the mechanisms necessary for the experiment.

Abstract

Alexander Ligman: Application of the Formal Design of Experiments to Deformed Airfoil Testing

(Under the direction of Dr. Nathan Murray)

Traditionally, one factor at a time (OFAT) testing is used to accomplish wind tunnel experimentation. OFAT testing is a process whereby one of the defined factors in the experiment is changed while all of the other factors are held constant. Afterwards, a new factor is chosen as the one to be manipulated, and the process is then repeated until all factors have been run through. Due to the possible cost-intensive and time-consuming nature of wind tunnel testing, formal design of experiments (DOE) has begun to be applied to wind tunnel experiments. In doing so, unique analyses can be made that elucidate such things as the interactive effects between factors and uncertainty within the experiment. The conversion to DOE from OFAT can be bothersome considering the need to understand how DOE can be applied to a new environment. The research objective was to apply the formal design of experiments to the wind tunnel testing environment to give a clearer understanding of how this application may be accomplished in future wind tunnel testing contexts. To do so, a load cell was used in the NCPA's low-speed wind tunnel to gather the lift and drag data of various deformed airfoils. Using this data, DOE analysis was performed to understand the relationships of the factors to the compiled data by using a 2-level fractional factorial design. Regression models were found for both the lift and drag. The drag model performed the best of the two. The lift response was shown to be reactive to multi-factor interactions, whereas the drag was not.

Table of Contents

List of Tables

List of Figures

1. Introduction

The traditional idea of experimentation involves the one factor at a time (OFAT) method. This is the changing of one independent variable while keeping the other independent variables constant. From this, data is gathered showing how the independent variable changes affected the sought responses. While comprehensive, if the number of factors becomes large, the cost of experimentation can grow rapidly. As such, cost-saving strategies are necessarily sought after, especially in the context of the aerodynamics testing environment, where physical testing can be a significant cost. Part of this cost is time requirements, where OFAT techniques can make the time needed to experiment greater than desired. This is especially true in light of the necessity of having to physically alter the wind tunnel environment for various different experiments. Often times, there is a substantial delay from when one experiment is run to the next due to this need. It is in this context that the potential benefits of the formal design of experiments (DOE) should be assessed (DeLoach, 2000).

The seminal introductory work to these experimentation methods was Ronald Fischer's text *The Design of Experiments*, published in 1935. While many industries have found good use of DOE, the aerodynamics industry has been slower to adopt such practices. Richard DeLoach applied DOE to prospective experiments at NASA's Langley High-Speed Wind Tunnel in 1997 (DeLoach, 1998). Since, more testing has been done using DOE with aerodynamic testing (English, 2007; Landman et al., 2002). The advantages of DOE lie in the reduction of the ratio of the data acquired to the information gained from said data. As compared to OFAT, by intelligently designing a test matrix, the resources required to perform an experiment can be theoretically, and often practically, reduced.

This is due to the fundamental principle that underlies DOE, as compared to OFAT. This is that DOE assumes that there are meaningful interactions between the variables being changed that manifest in the response measurements (Coleman & Gunter, 2014). Due to OFAT's limitations, this principle is inherently not being tested. As such, these effects are not understood. This is an avenue through which the ratio of data to information is optimized. As given the same number of trials, comparisons can be made internally to discover main effects, but also interactions of variables. This is contrasted to OFAT, where only the main effects of changing a variable could possibly be determined.

At this point, it is useful to understand the basics of DOE so that they can later be applied to an experiment. There are definitions to understand more formally than they have been applied so far. Starting out, there are "factors." These are "experimental variable[s] that [are] changed in a controlled manner" (Coleman & Gunter, 2014). These factors have "levels" which are the values of said factors. The "responses" are the measured outcomes of the experiment. A single "run" is a set where all factors have a defined level. And the "design" is the combination of all runs understood as a collective. For example, the meaning of a four-factor, 2-level design with sixteen runs should be clear. A note on the number of runs: while it is seen in the previous example that there is a relationship between the number of runs and the factors and levels (number of levels taken to the power of the number of factors equals the number of runs), the exact number of runs is a question with nontrivial implications that will be discussed later.

With this terminological framework set, there three overarching components to DOE to understand (English, 2007). The first of which is randomization. This is a hallmark of the scientific method in general and, as such, is applied to DOE as well as OFAT methods. The benefit of randomization is found in the removal of the effects of extra-experimental factors that could affect

the outcome of the experiment. In terms of its application to DOE and for the purposes of this paper, randomization takes the form of randomizing the run order of the sequentially performed experiments.

The second component is blocking; this is a reduction of true randomization. This is when certain experimental runs need to be grouped together due to the constraints imposed by the testing apparatus. For example, this could result in the number of runs in an experiment being divided into two parts, where part one gets performed on day one, and part two on day two; in this example, the ambient conditions of said experiment may affect the results from day to day and therefore need to be accounted for. Essentially, the blocks become another variable to be accounted for, the effects of which are factored out in the data analysis.

The last component is replication, another hallmark of the scientific method in general. Simply, this is where runs are repeated with factors at the same levels but using novel factors. This means that for a true replicate, the factor and level selection must be independent of the previous run other than for the nominal values.

2. Methodology

In seeking to apply DOE to an aerodynamic testing environment, the goal of the experiment was first determined. In seeking to under how deformation affects various aerodynamic capabilities of varying airfoils, researchers often have to physically apply the deformation to a scale model of the airfoil and then perform a test wherein they gather the necessary data to see how the airfoil is affected by the deformation as compared to a naked airfoil (Ignatyev et al., 2020). Due to the physical necessity of applying deformation, it was seen that being able to reduce the amount of resources required for understanding the deformation effects would be desirable. As such, this kind of testing was considered a good candidate for applying an exploratory DOE experiment.

In doing so, it was necessary to determine a quantitative way to apply deformation to the airfoils so that a consistent analysis could be accomplished. By reviewing deformation impact testing literature, components of this definition were found: namely, that the depth of the indentation and the radius at the surface of the impacted plate were two quantitative factors to be used (Calder, 1971). The deformation of an airfoil has been understood in a similar light as the indentation depth from the original profile (Sun et al., 2021; Tatlıer & Baran, 2020). With these two factors determined, the other necessary factors were decided based on the remaining need to fully define the deformation; this need was primarily that there needed to be a way to place the deformation somewhere on the airfoil. As such, the distance along the chord that the tip of the indentation sat at was determined as the third factor. Similarly, the distance that the tip of the indentation sat along the cross-sectional direction of the airfoil was determined as a fourth factor.

With these four factors having been defined, more were considered, such as the gradient from the airfoil surface to the point of indentation, and the profile that the gradient followed. A

design decision was necessary regarding this. Adding one or both of these factors would have had the benefit of more completely defined deformation. But, as was elaborated upon earlier, since the number of runs for an experiment is based on a power of the factors, adding more factors quickly increases the necessary number of runs. As such, the four initial factors were decided upon as the most necessary for accomplishing the definition. Further, the responses were also determined. As it was of interest to discover how the deformation affected the aerodynamic capabilities of the airfoils, the responses chosen were those that are used ubiquitously to determine such capacities; these being lift and drag.

Table 1: Factor Definitions

Factor	Definition
1	Length along Chordal Direction
2	Length along Cross-Sectional Direction
3	Diameter of Indentation
4	Depth of Indentation

This led to the determination of the exact kind of experiment that was going to be run. A full factorial experiment is one wherein there are all of the combinations of the levels of the factors present. These kinds of experiments are ideal as they allow for determining factor interaction effects. The number of runs that determine of a full factorial experiment is determined by the number of levels to the power of the number of factors. While it is possible to reduce the number of runs, thereby creating a fractional factorial, difficulties arise in data interpretation.

This is due to aliasing. Aliases arise from the fact that within the fractional factorial test matrix there are combinations of factors that are changing together in the same way (increase/decrease). As such, it becomes difficult to draw conclusions about the factors severely affected by aliasing. By severe affectation, it is meant that the factor or factor combination of

interest is aliased with a two-factor interaction. Being aliased with a three-factor interaction is more acceptable, as much more rarely do three factors exhibit a statistically important collective effect on the response and, as such, can be disregarded. But, two-factor interactions are much more likely and so if a response is aliased with this, it becomes difficult to parse whether the measured response is due to aliasing effects or the response of interest (Anderson & Whitcomb, 2015).

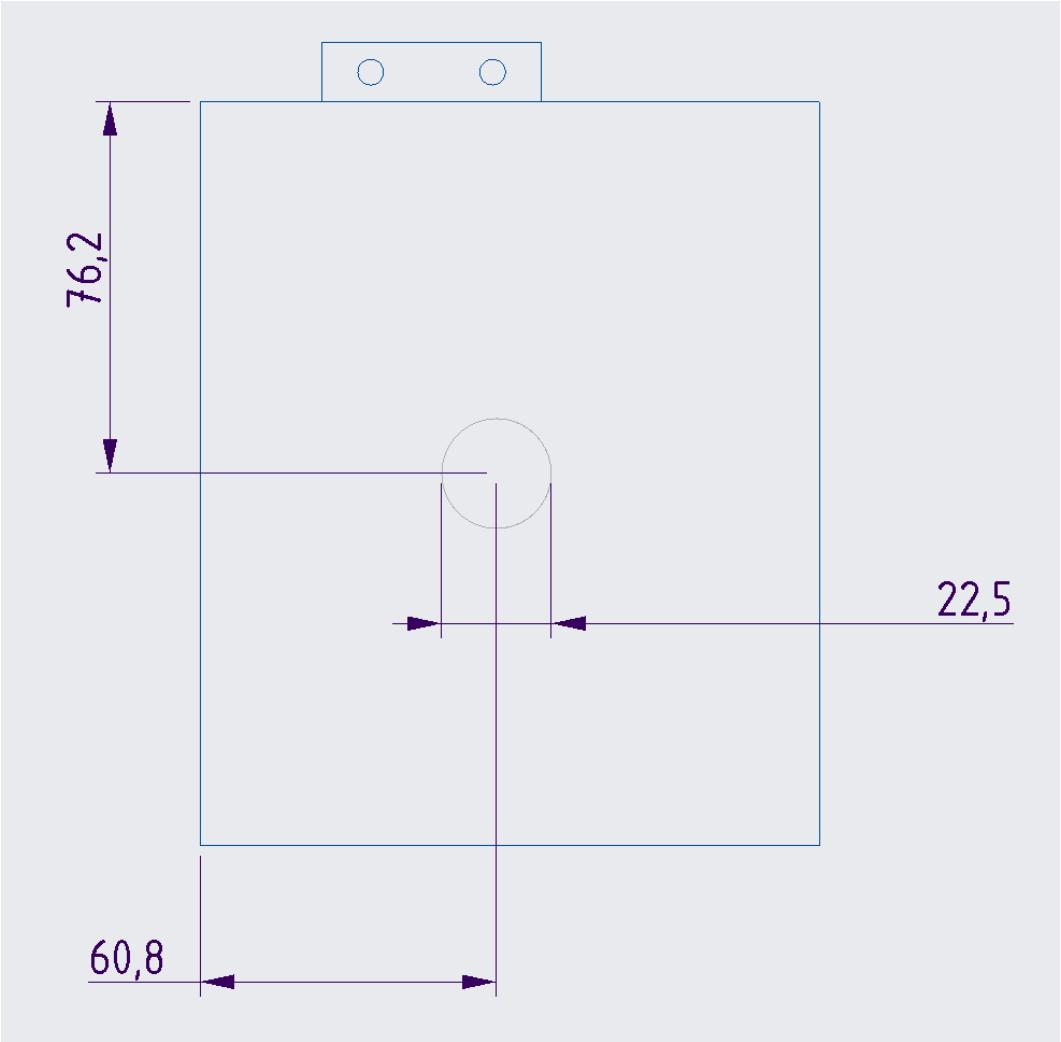

Figure 1: Example of Factors 1-3

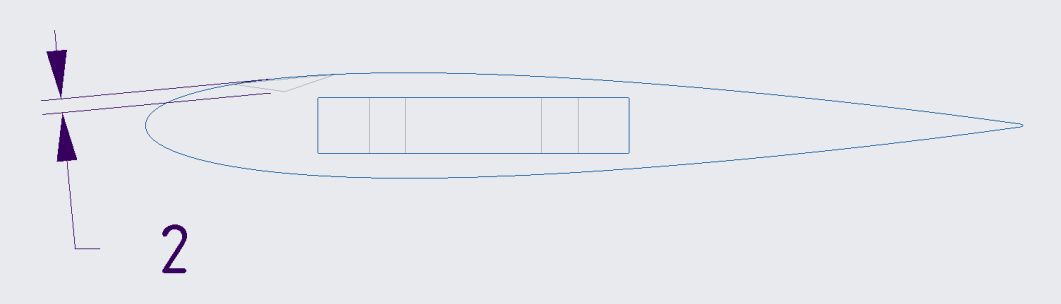

Figure 2: Example of Factor 4

As such, the information-cost tradeoff must be examined and understood. As for this experiment in particular, due to the cost of manufacturing airfoils for each combination of factors in the test matrix, it was desirable to minimize runs if possible. This being the case, it was determined that a full-factorial experiment of sixteen runs would be cost-prohibitive. Therefore, a resolution four fractional factorial design was chosen. This was to keep to the four factors already determined and still be able to determine some useful information from the experiment. This would allow for understanding the main effects and possibly determine the existence of interactions; this kind of experiment is more formally considered a screening experiment. It was reasoned that this would be sufficient to accomplish the goals set forth. This meant that instead of sixteen runs, eight would be used; the substantial cost savings are highlighted here, reducing by half the amount needed to run the experiment.

With this determined, the design matrix was subsequently found. As this is just a blank matrix showing the arbitrary levels of the factors (“0” for a low value and “1” for a high value), the necessary levels were going to need to be determined. Ideally, the values chosen for the low and high settings would be far apart from one another so that the effects of the factor in question could be more easily examined. As such, this was accounted for. For the first two factors that place the damage spatially on the airfoil, the values of the last two factors needed to be taken into

account. This is due to the fact that if the diameter of the damage profile was at its high value, and one of the spatial factors was also at its high value, it was possible that the damage profile would actually exceed the boundary of the airfoil. As such, the maximum diameter and depth were determined first. These factors were also limited but in different ways.

Table 2: Blank Design Matrix

Run (Standard)	Factor 1	Factor 2	Factor 3	Factor 4
1	0	0	0	0
2	1	0	0	1
3	0	1	0	1
4	1	1	0	0
5	0	0	1	1
6	1	0	1	0
7	0	1	1	0
8	1	1	1	1

Part of the limiting factors were the physical dimensions of the airfoil. A compromise between fitting the airfoil into the wind tunnel but also having enough surface area and volume to sufficiently damage the airfoil was necessarily made. As such, the chord length was decided to be 127 mm (5 in) and the width of the airfoil was determined to be 152.4 mm (6 in). The NACA 0012 profile was scaled to these dimensions.

Due to the ever-changing spline that defines the edge of the airfoil's cross-section, applying a flat shape to the airfoil grew increasingly difficult as the shape became larger. As such, any sufficiently large hole diameter would be distorted from the circular shape to an undesirable amount. Due to this, 30 mm was considered the maximum diameter. At this diameter the circle only showed a discrepancy between two perpendicular diameters of 0.2 mm. The minimum diameter was set at half of this value, so 15 mm. This was done to ensure that a large enough

minimum profile would be applied to affect a change on the airfoil substantial enough to see a change in the airflow. The original design for the minimum target was 10 mm, but it was deemed to be too small. Having determined the diameter values, the length factor values were then determined, again with a primary focus on separating them as much as possible. After this, the maximum depth was determined based on the area of the airfoil with the smallest cross-section. This limited the maximum depth to 5 mm. The minimum was then set at 2 mm to increase the range as much as possible. With all of the values determined, a finalized design matrix was implemented. It was from this that each of the airfoils was designed.

Table 3: Filled Design Matrix

Run (Standard)	Factor 1	Factor 2	Factor 3	Factor 4
1	20	25.4	15	2
2	101.6	25.4	15	5
3	20	127	15	5
4	101.6	127	15	2
5	20	25.4	30	5
6	101.6	25.4	30	2
7	20	127	30	2
8	101.6	127	30	5

3. Experiment

The experiment was to take place in the low-speed wind tunnel at the National Center for Physical Acoustics. To measure the lift and drag forces on the airfoil, a Mini-58 Six-Axis Force/Torque Sensor System load cell was used. Due to the novel nature of the airfoil testing, various mounting components had to be designed. Of primary importance, the airfoil had to be attached to the load cell in a sufficient manner to enable the reading of measurements. Further, a method for enabling angle of attack (AoA) changes was desired so that further comparisons could be made. There was an initial design considered. While this design technically achieved the goal of mounting the airfoil to the load cell, there was a significant issue with it. The Mini-58 load cell measures the reaction forces of the attached airfoil; as such, adding a pin on the back of the airfoil to ensure stability added a second reaction force, one that the load cell could not account for. As such, a second, final design was initiated; this one being based off previously used designs at the NCPA. This design ensured that the airfoil was designed in such a way that it was only connected to the load cell; this was accomplished by using an adapter plate. Further, to cover the goal of needing to change the AoA, a knob that could be manually rotated was designed to be attached to the bottom of the load cell. Figures 3, 4, and 5 show the experimental setup.

Figure 3: Experimental Setup

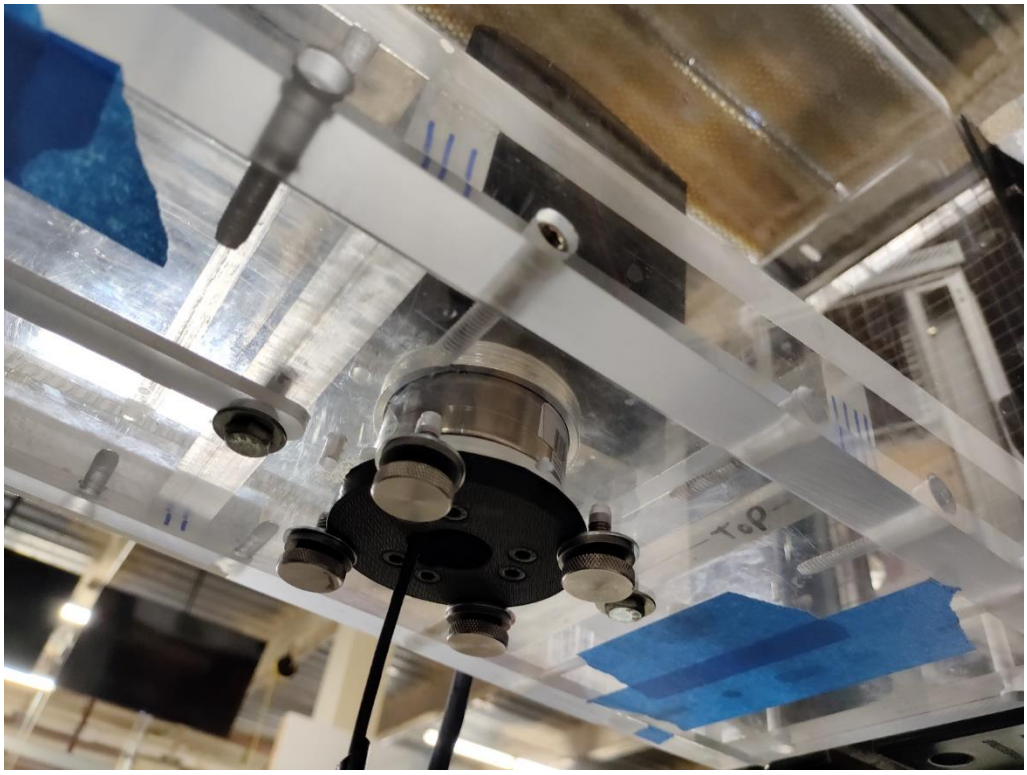

Figure 4: AoA Adjustment Mechanism

Figure 5: NCPA Low Speed Wind Tunnel

The design work was accomplished using the student license of Creo Parametric. After modeling all necessary parts, the parts were sent for manufacturing to the 3-D printing company Xometry. Further, mounting hardware such as screws and pins were sourced using McMaster Carr. To facilitate the use and understanding of formal DOE, the widely used Design Expert™ software was used.

The experiment was to be run at the maximum wind tunnel speed achievable, which was an average of 37 feet per second. This was the capability of the wind tunnel. The test was run at maximum speed to ensure that the responses could overcome the noise of the load cell drifting. For instance, at 0 degrees AoA and a low wind speed, the measured drag and lift values were small enough that load cell drift could have overcome the response entirely, not only just marginal changes in the response between runs. As a result, the decision to run the test at maximum speed

was made; for similar reasons, the DOE runs were run at 15 degrees AoA. Further, a correction factor was put into the data processing that attempted to correct for any load cell drift.

As to why this drift came about, the specific load cell used in the experiment was temperature-sensitive. As such, over the course of testing, the load cell heats up/cools down, which causes small expansions/contractions; the movement is then registered in the load cell as changes in the forces applied to it. To correct, a baseline was taken on the first run of the load cell after zeroing it, and then this correction factor was applied to every subsequent run, relative to the amount of drift that the specific run in question demonstrated; this is illustrated in table 4, which shows the process for the raw 'F_x' values recorded from the load cell. This same process was done for 'F_y' and 'F_z.' The correction factor was the mean value of the responses while the wind tunnel was off that were being measured before the first run; this run was done immediately after zeroing the load cell for the experiment, and as such represented the load cell values without any drift. The mean value of a similar interval before the wind tunnel was turned on was taken for each subsequent run as well. Then the subsequent runs were shifted to correct for the difference in values while the wind tunnel was off, the drift.

Table 4: Attempted Drift Correction

	Raw 'F_x' Data		
Run	Initial (Global) Bias	Local Drift	Applied Bias
1	0.0119	0.0119	0
2	0.0119	0.2221	0.2102
3	0.0119	-0.1487	-0.1606
4	0.0119	-0.2964	-0.3083
5	0.0119	-0.2865	-0.2984
6	0.0119	-0.5554	-0.5673
7	0.0119	-0.1649	-0.1768
8	0.0119	-0.4760	-0.4879
9	0.0119	-0.6940	-0.7059

As table 4 shows, the global bias was the same for all of the corrections. This is the average value read by the load cell over 500 samples when the tunnel was off, right after zeroing it before any testing began. The local drift is the average of over 500 samples before the tunnel was turned on for every run. The bias is then applied to the data found with equation 1. This served to shift the data to eliminate the differences between the wind tunnel off, steady-state values, which was assumed to be due to the temperature drift. The applied bias was then applied to the data set in question.

$$\text{Applied Bias} = \text{Local Drift} - \text{Initial Bias} \qquad \text{eq. 1}$$

While this corrective action was taken, it should not be considered to be sufficient insofar as the actual temperature curve that effects drift in the load cell is a logarithmic curve; as such, this curve behavior specifically needs to be accounted for and subtracted out. For the purposes of simplifying the data interpretation, this is simply noted as needing to be investigated and fully accounted for in future studies.

Lastly, originally an angle of attack sweep from -10 to 10 degrees was going to be performed to gather a more holistic picture on the performance of the airfoil, not necessarily to add to the DOE component of the experiment. But, in testing the wind tunnel before running the experiment, it was found the usable angle of attack sweep was from 5 to 15 degrees. There was an effect present that severely disrupted data collected for any angle of attack that was outside of this range. This effect was presumed to be some kind of wall effect, as the airfoils used were relatively large when compared to the internal space of the wind tunnel. Further, it was noticed that outside of the usable range of AoA, there was a distinct whistling sound made by the tunnel. The effect was experienced by both deformed and undeformed airfoils over the AoA range.

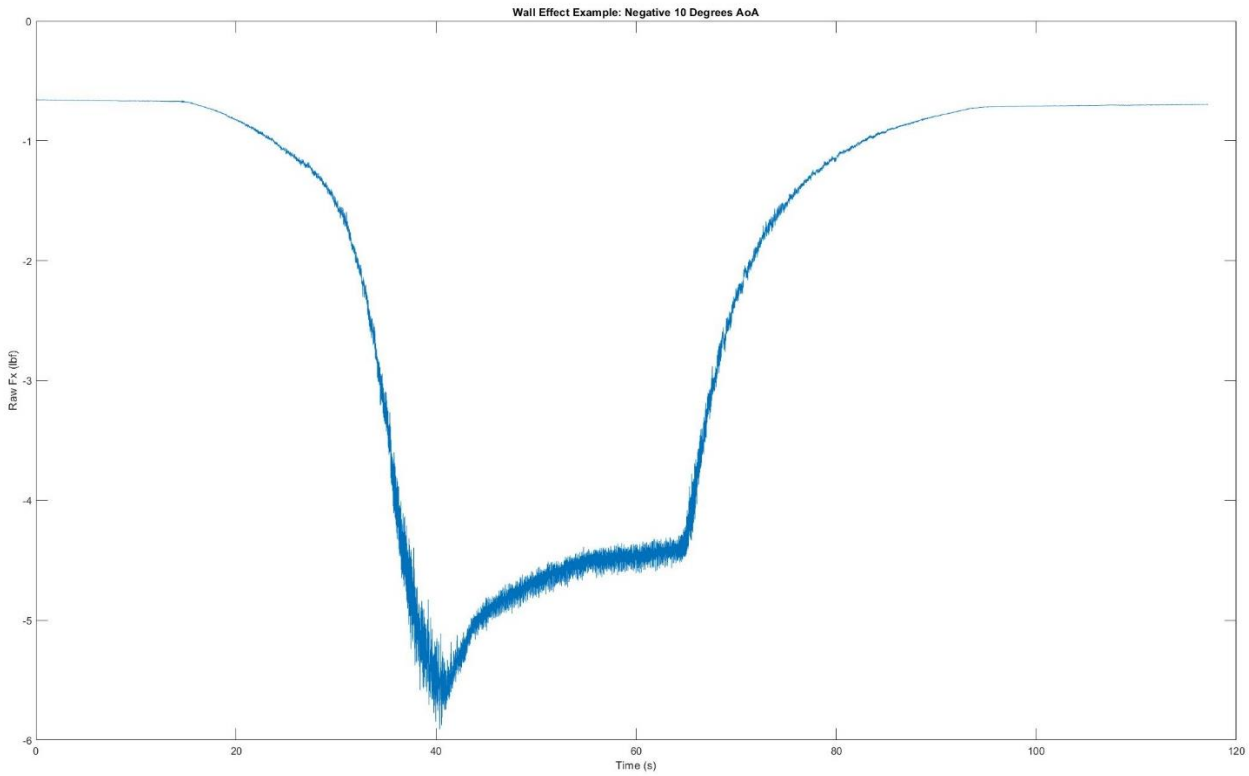

Figure 6: Negative 10 degrees with Undamaged Airfoil

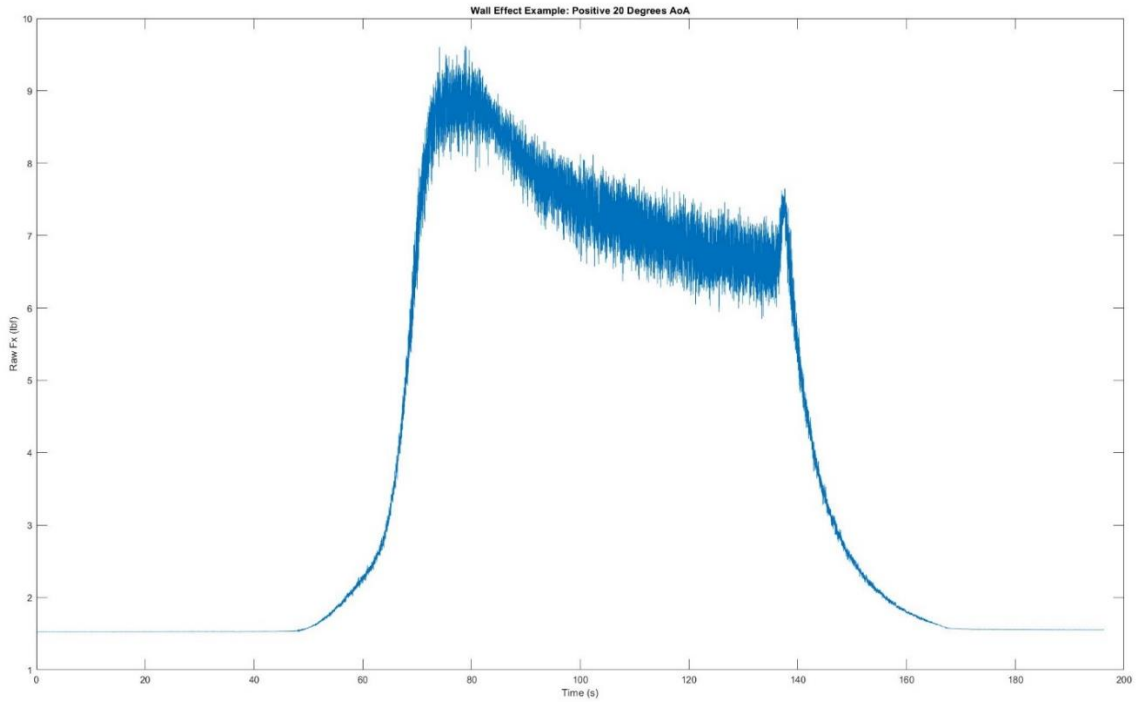

Figure 7: Positive 20 degrees with Damaged Airfoil

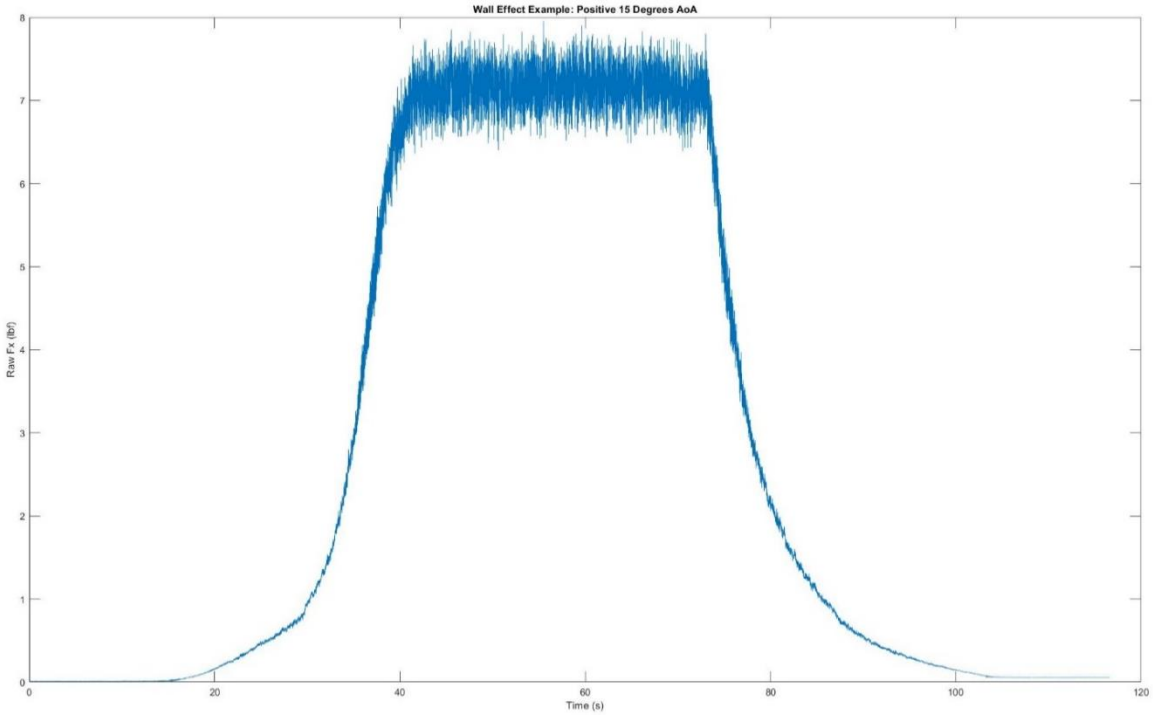

Figure 8: Actual Test Data of Damaged Airfoil at 15 degrees

4. Results

The results are shown in table 5. The highlighted run is the center point value that was used to test for curvature. The lift analysis is shown in the following figures. The half-normal plot in figure 9 was used to determine those factors and affects that would go into the model. The plot is used as a visual tool to select the factors, where the red line represents data more likely to be noise, or at least indistinguishable from experimental noise, while those points not along the line are more likely to be experimental signal. As such, the largest effects, the most to the right, are selected until the points most to the left all fall along the red line (Kraber, 2021).

Table 5: DOE Run Data

Run	Drag (lbf)	Lift (lbf)
1	-4.870888183	9.88362566
2	-4.844867805	9.822342011
3	-4.874152453	9.87064066
4	-4.899492025	9.811880592
5	-4.870212406	9.932625544
6	-4.85020965	10.07338781
7	-4.82361902	9.901639661
8	-4.845660823	9.832748183
9	-4.848632973	9.913569758

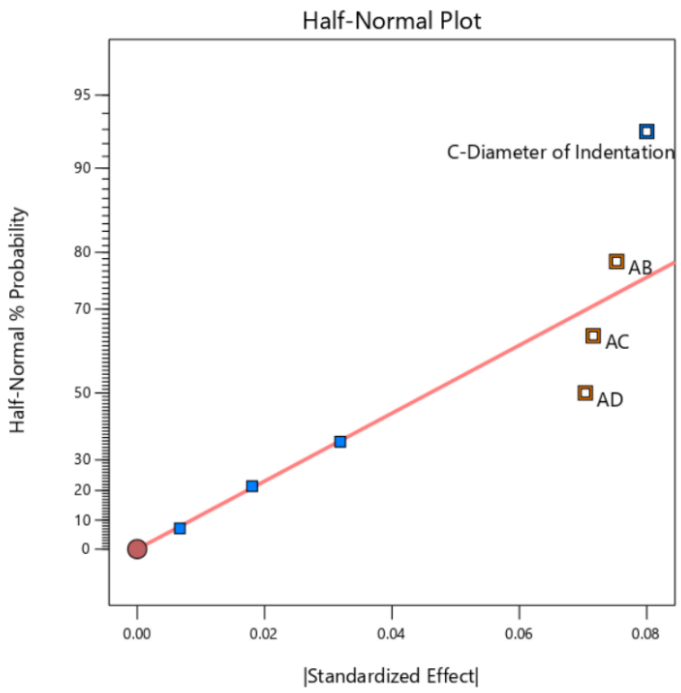

Figure 9: Data Selection for Lift Model

From figure 9, the selected data was the diameter of indentation and the interaction of AB, AC, and AD. Further below, tables 6 and 7 give important statistical values of the lift model. The F-value is a statistical test whereby the model in question is compared against a model that is based only on the mean value of the data set. The p-value shows the percent chance of the observed and modeled relationship being due to noise and for significance $p < 0.05$. As such, with a p-value of 0.0130, there is a 1.30% chance that the F-value of 13.85 could occur due to noise.

Table 6: Lift Analysis of Variance

Source	Sum of Squares	df	Mean Square	F-value	p-value	
Model	0.0470	4	0.0118	13.85	0.0130	significant
C-Diameter of Indentation	0.0136	1	0.0136	16.02	0.0161	
AB	0.0120	1	0.0120	14.18	0.0197	
AC	0.0109	1	0.0109	12.83	0.0231	
AD	0.0105	1	0.0105	12.39	0.0245	
Residual	0.0034	4	0.0008			
Cor Total	0.0504	8				

Table 7: Lift Model Fit Statistics

	Std. Dev.	0.0291		**R^2**	0.9327
	Mean	9.89		**Adjusted R^2**	0.8654
	C.V. %	0.2944		**Predicted R^2**	0.5972
				Adeq Precision	10.7675

It should be noted that the predicted R^2 and adjusted R^2 are further apart than 0.2. This can imply many things, but it further impresses the need for confirmation runs to ensure that the model is accurate, as these R^2 can suggest bad data. The adequate precision is sufficient, as 10.7675 > 4. Lastly, the inclusion of a center point value showed that there was no significant curvature for the model, and as such for the analysis it was discarded. Figure 10 and figure 11 show the residuals of the modeling.

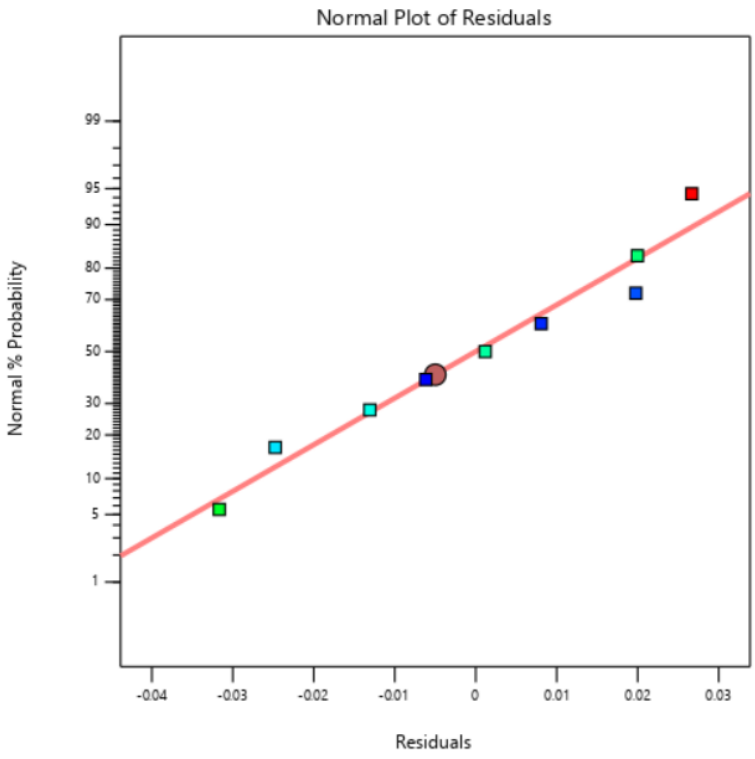

Figure 10: Lift Normal Plot Residuals

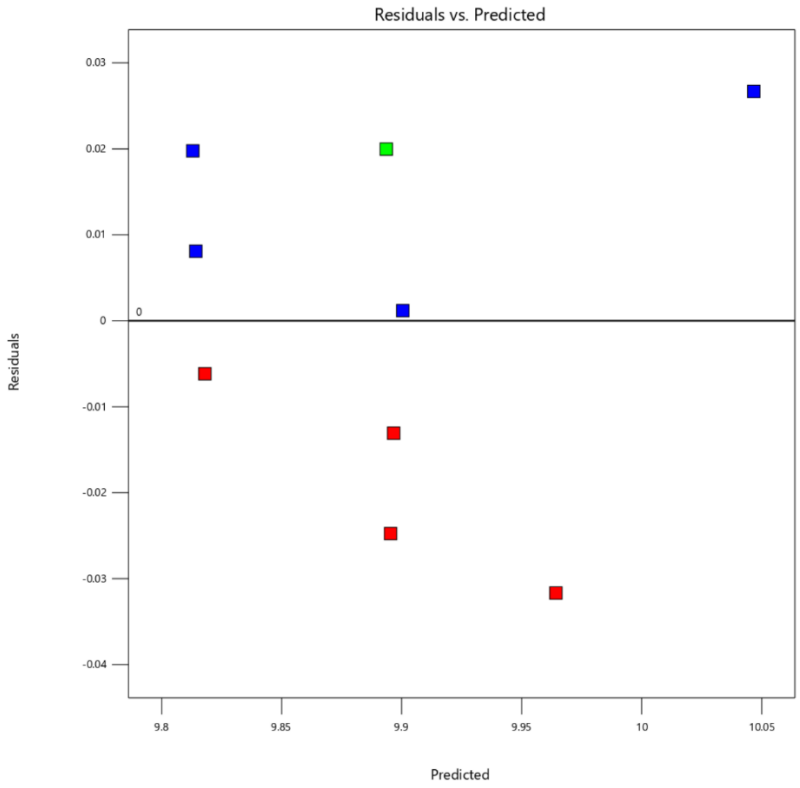

Figure 11: Lift Residuals versus Predicted

The normal plot of the lift residuals shows good behavior; the residuals versus the predicted shows more erratic behavior than would be ideal, again showing the need of confirmation runs before anything definitive could be said regarding the model. Ideally, the vertical spread of the residuals should be roughly constant from left to right; an increase in the residuals from left to the right can indicate a non-normal error. Figure 12 shows the model's prediction versus the actual data acquired. If the model perfectly fits the experimental data, then all points would fall along the black line as the actual value would be equal to the predicted values. It can be seen that not all points fall along the line, but they are all grouped near it. Figure 13 shows how the chosen factors influence the lift. Considering that of the original factors, only the diameter of indentation was chosen, this is the only plot present. Equation 2 represents the coded equation for lift.

$$\text{Lift} = 9.89 - 0.0412(C) + 0.0388(AB) + 0.0369(AC) + 0.0362(AD) \qquad \text{eq. 2}$$

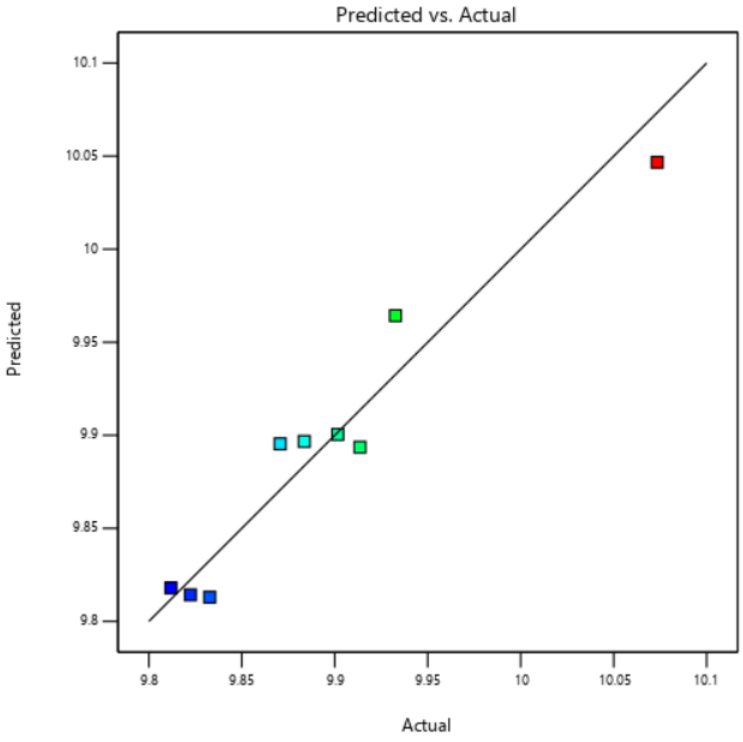

Figure 12: Lift Model versus Experimental Data

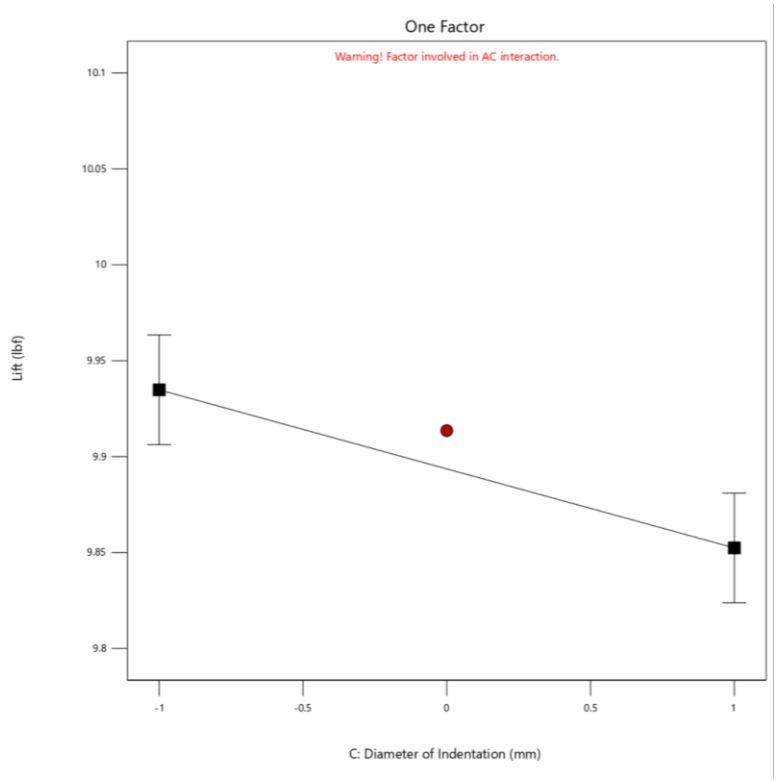

Figure 13: Model factor effect on Lift Response

Figure 13 shows that as the diameter of the indentation increases, the lift reduces. Similarly, the lift is maximized whenever the diameter of indentation is the smallest. This coheres with the assumption that the greater the damage to the airfoil, the more the air will be disturbed and, therefore, the greater the lift will be affected. Figures 14, 15, and 16 show the interactive effects between AB, AC, and AD respectively. The lines on the figures represent the factor labeled at the top; one line represents this factor at its low level, and the other at its high level. Interactions can be seen to be relevant if the lines are not parallel.

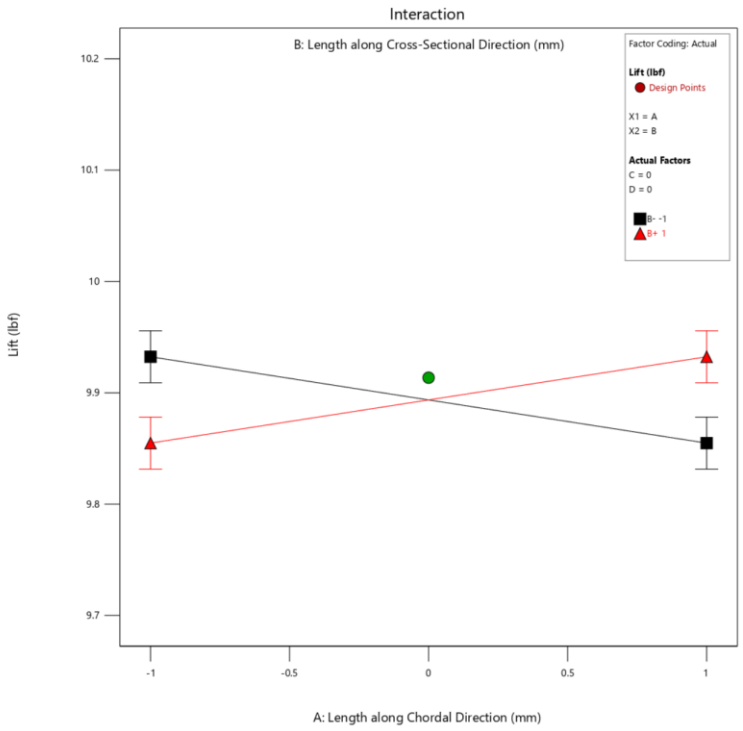

Figure 14: Interaction Plot of Factors A & B

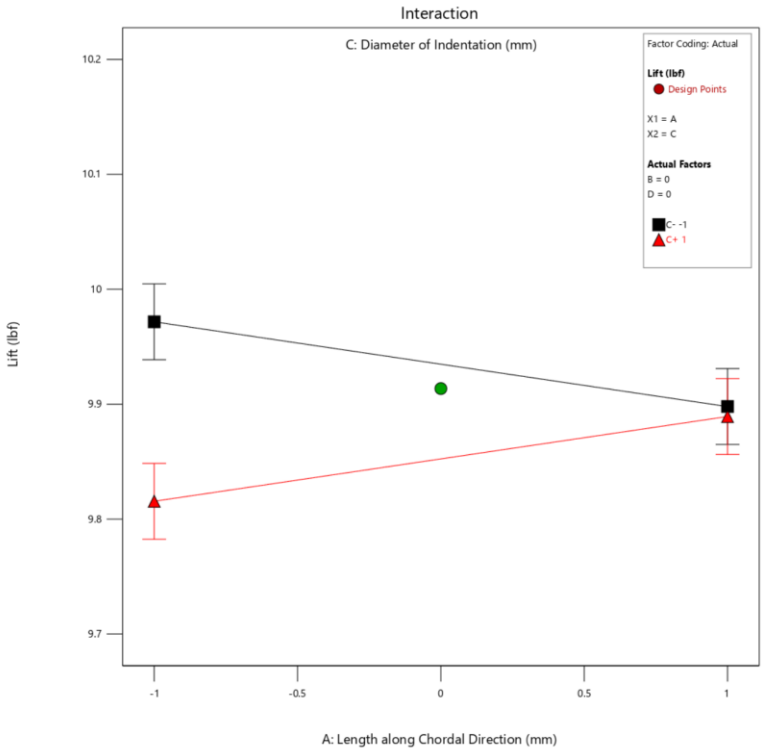

Figure 15: Interaction Plot of Factors A & C

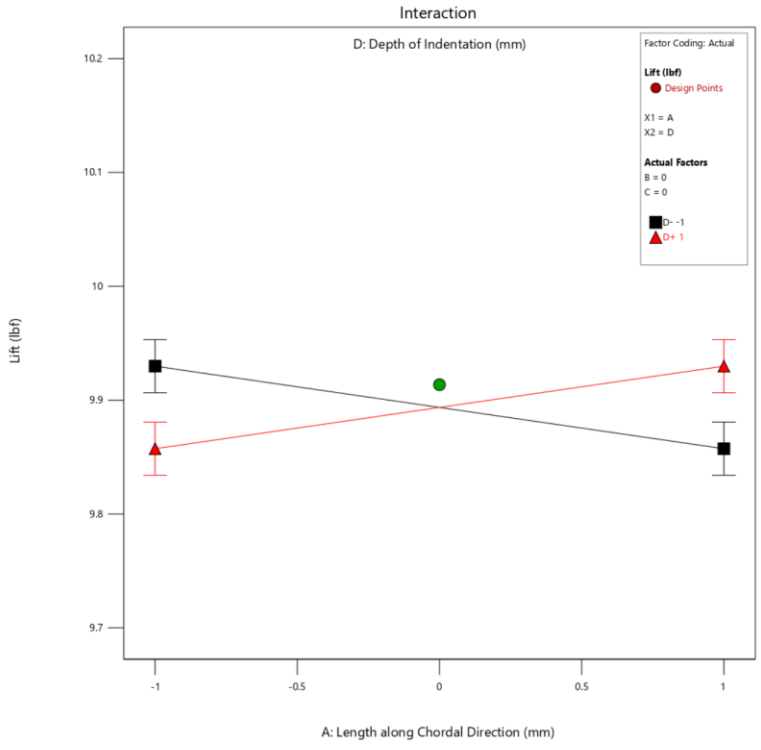

Figure 16: Interaction Plot of Factors A & D

As is the case in figures 14 and 16, it can be seen the interactions AB and AD are both relevant over the entire range of the levels; this is demonstrated by the points at the ends of the lines being separated from one another. Although, since the lines switch and mirror each other, this means there are no main effects caused by B and D. This confirms the half-normal plot selections earlier where neither B nor D were selected as main effects. Further, this principle is applied to Figure 15, where not only are there interactive effects between factors A and C, but also C shows itself to be the main effect in that the differences between the two ends of the lines have different absolute values.

After completing the lift analysis, a similar analysis was performed for the drag. Figure 17 shows the factor selection for the model. This plot was more typical as would be expected of a half-normal plot. For the drag main effects, all four of the original factors were selected as significant, but none of the interactions were found to be significant.

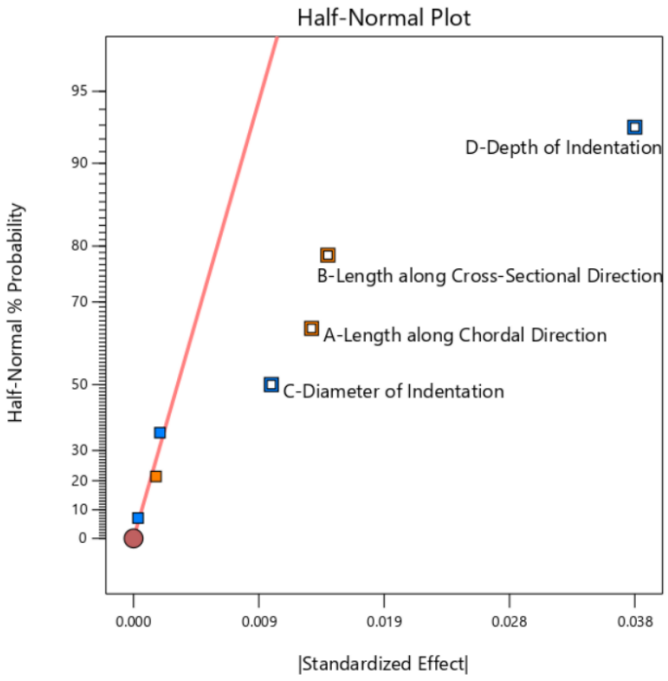

Figure 17: Data Selection for Drag Model

Tables 8 and 9 show the analysis of variance and fit statistics for the drag model, respectively. As was suspected from the half-normal plot, the F-value of the drag model was much higher, showing a better fit. Similarly, the p-value was lower as well. Both values were significant, and for the drag model, there was a 0.05% chance that the F-value of 207.73 would occur due to noise. For this model, the R^2 values are closer together, indicating a much better model fit for the drag model than for the lift model. Again, the adequate precision value of 43.3211 > 4 and so is sufficient. Lastly, another difference from the lift model: the center point value suggested that there was significant curvature present in the model. As such, this was factored into the model. Figures 18 and 19 represent the drag residuals.

Table 8: Drag Analysis of Variance

Source	Sum of Squares	df	Mean Square	F-value	p-value	
Model	0.0038	4	0.0010	207.73	0.0005	significant
A-Length along Chordal Direction	0.0004	1	0.0004	77.50	0.0031	
B-Length along Cross-Sectional Direction	0.0004	1	0.0004	92.43	0.0024	
C-Diameter of Indentation	0.0002	1	0.0002	46.46	0.0065	
D-Depth of Indentation	0.0028	1	0.0028	614.52	0.0001	
Curvature	0.0001	1	0.0001	24.48	0.0158	
Residual	0.0000	3	4.601E-06			
Cor Total	0.0039	8				

Table 9: Drag Fit Statistics

Std. Dev.	0.0021		**R^2**	0.9964
Mean	-4.86		**Adjusted R^2**	0.9916
C.V. %	0.0441		**Predicted R^2**	NA[(1)]
			Adeq Precision	43.3211

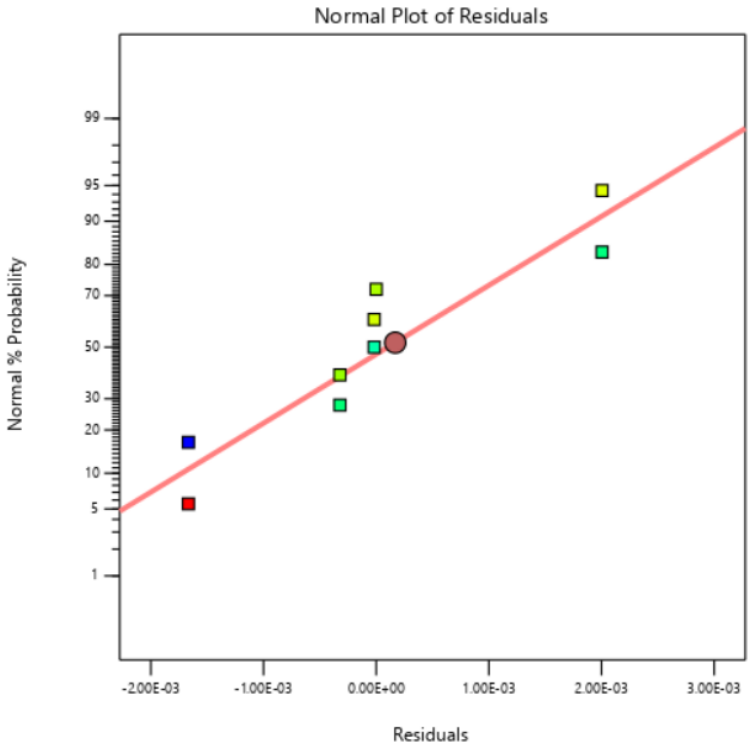

Figure 18: Drag Normal Plot Residuals

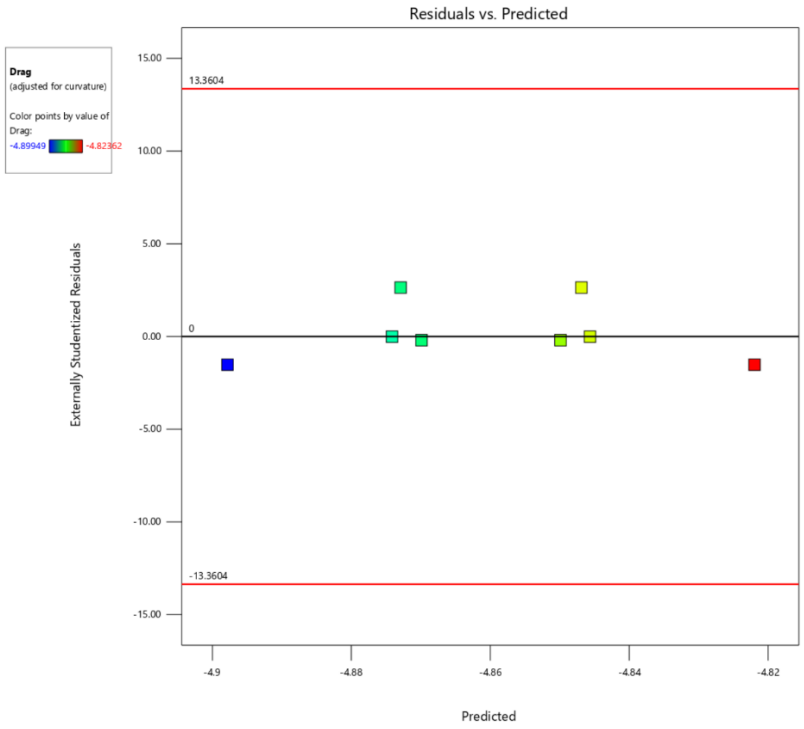

Figure 19: Drag Residuals versus Predicted

As can be seen from the drag residuals, they fall along the lines that were expected. Although not perfectly ideal, they suggest the behavior that is sought of residuals. Figure 20, below, shows the prediction of the drag model versus the actual data. It can be seen that the real data points mostly fall on the line predicted by the model. This explains the high R^2 values for the drag model. Due to the drag being a hierarchical model, both a coded and actual equation were obtained and are shown in equations 3 and 4 respectively.

$$\text{Drag} = -4.86 + 0.0067(A) + 0.0073(B) - 0.0052(C) - 0.0188(D) \quad \text{eq. 3}$$

$$\text{Drag} = -4.85989 + 0.006676(A) + 0.007291(B) - 0.005169(C) - 0.0188(D) \quad \text{eq. 4}$$

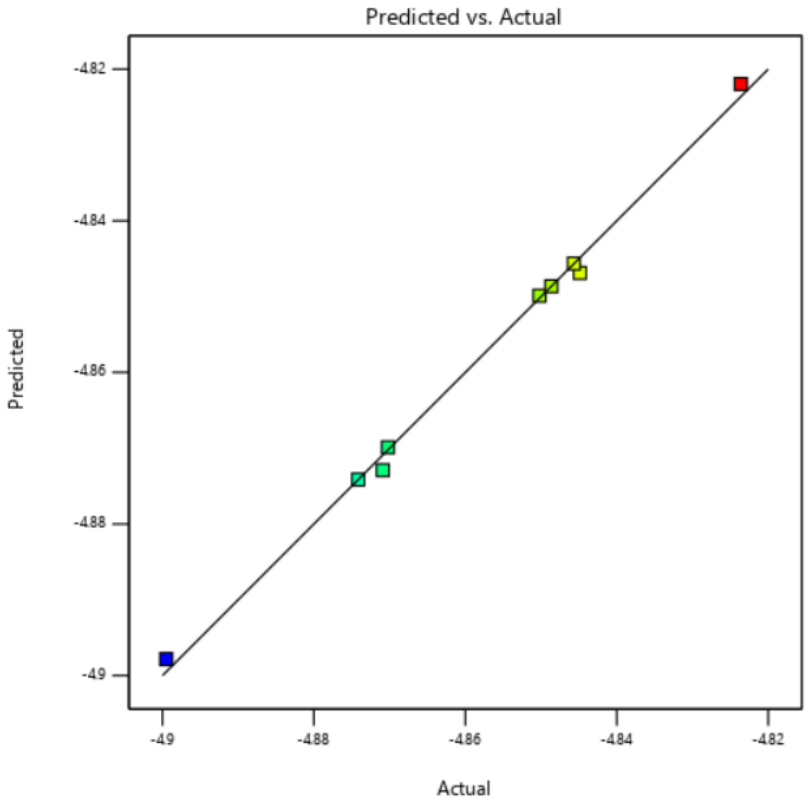

Figure 20: Drag Model versus Experimental Data

Figure 21 represents the effects of the model factors on the drag response. It can be seen that when factors A and B are at their low levels, meaning the damage profile is most near to the upstream root of the airfoil, the drag is maximized (when examining the absolute value). For factors C and D, when they were maximized, so was the drag. This meant that the 'larger' the deformation of the airfoil, the more drag it experienced.

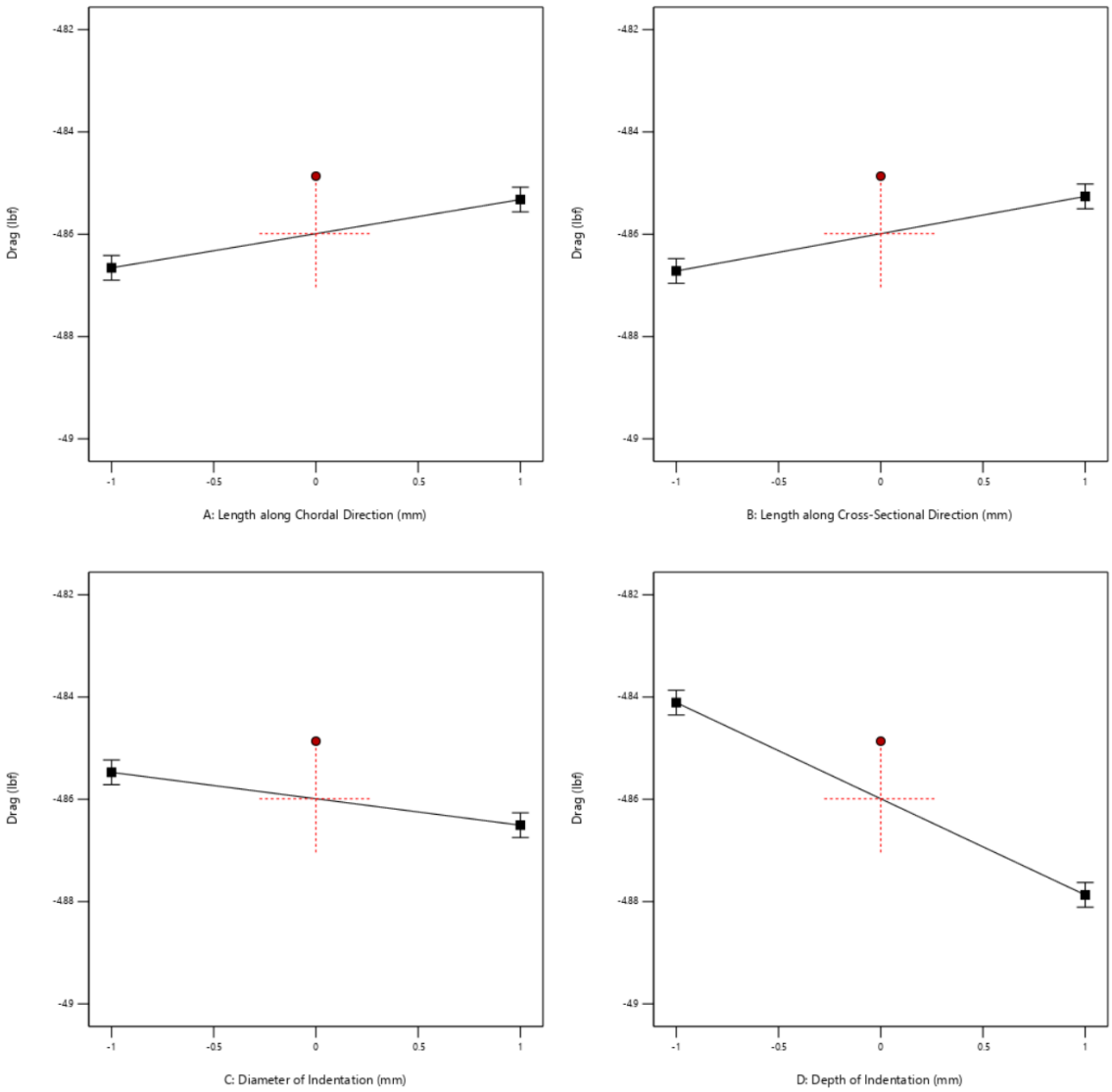

Figure 21: Model factor Effects on Drag Response

5. Post Results Analysis

Using the models, various optimizations were performed to investigate how the predictive prowess of DOE could be applicable in future scenarios. Figure 22 shows the optimization where the lift is being maximized above all else. Figure 23 is an optimization where drag is being minimized above all else; in this case, the specific input was to 'maximize' drag as the drag values were negative according to the direction of the force applied to the airfoil.

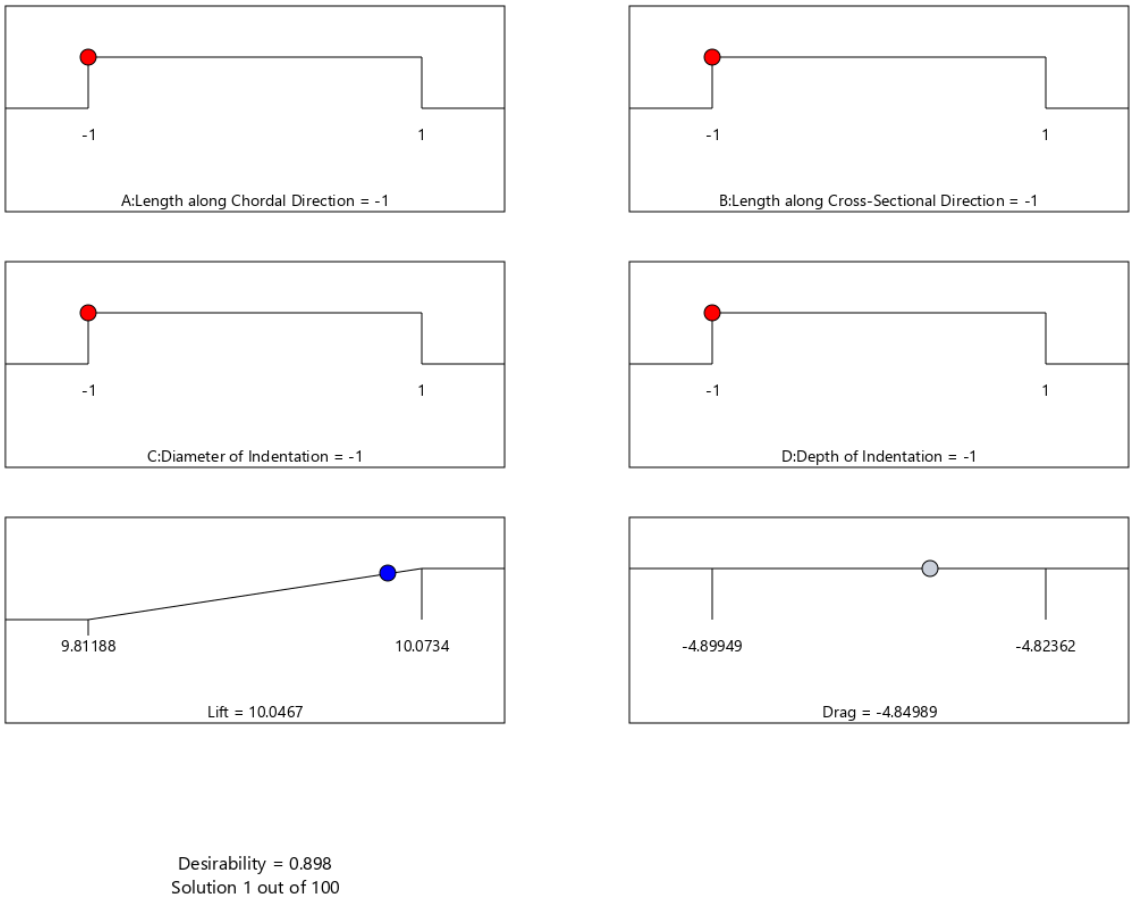

Figure 22: Lift Optimization

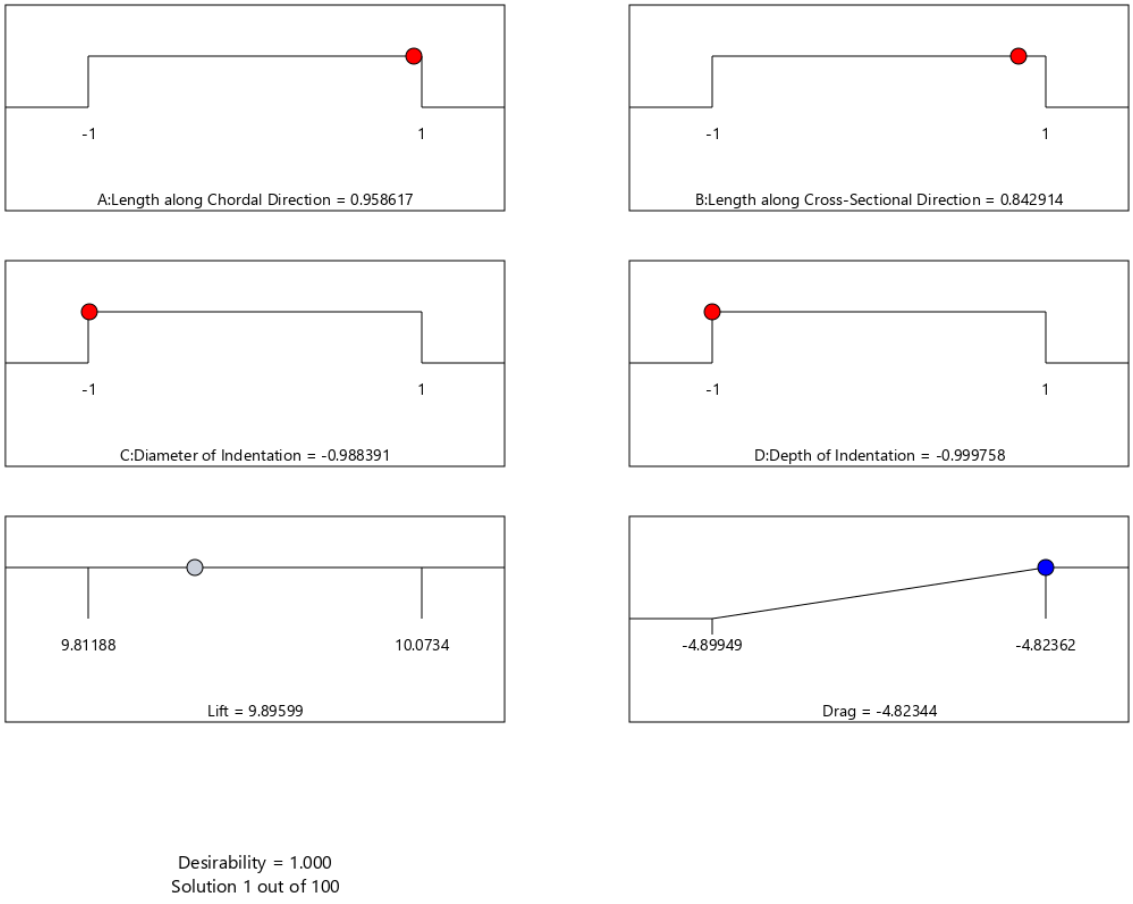

Figure 23: Drag Optimization

The lift optimization further showed the poor fit of the model. This is due to the fact that it could not replicate the maximum lift that actually occurred during experimentation when the levels were set to the same nominal values. The drag optimization performed better, again on account of the model being a far better fit of the data. As such, this optimization gives a desirability of 1.000, the best possible. It also shows how the various factors need to be set: the location of the damage needs to be far from the root and upstream side of the airfoil within the model domain; the size of the damage needs to be minimized, with a small diameter and small indentation.

6. Conclusions

An exploratory study on applying the formal design of experiments to the wind tunnel environment was complete. A wind tunnel experiment involving deformed airfoils was successfully defined and a formally designed experiment in the form of a 2-level fractional factorial was attempted and completed using the NCPA's low-speed wind tunnel. Using statistical analysis, regression models of both lift and drag were determined. It was determined that there were serious interactive effects that fed into the lift, but determining the exact relation due to aliases became difficult. Further, the lift model showed a poorer fit as compared to the drag model. The drag regression model included all of the original factors and suggested no important interactive effects between them. Also, it was determined that the drag regression had a significant curvature to it due to the inclusion of a center point in the experimental runs. Lastly, an exploratory optimization analysis was completed to further elucidate the potential benefits of using formally designed experiments.

BIBLIOGRAPHY

Anderson, M. J., & Whitcomb, P. J. (2015). *DOE simplified: Practical tools for effective experimentation* (Third edition). CRC Press, Taylor & Francis Group.

Calder, C. A. (1971). Plastic deformation and perforation of thin plates resulting from projectile impact. *Int. J. Solids Structures*, *7*, 863–881.

Coleman, D., & Gunter, B. (2014). *A DOE Handbook: A simple Approach to Basic Statistical Design of Experiments*. CreateSpace Independent Publishing Platform.

DeLoach, R. (1998, January 12). Applications of modern experiment design to wind tunnel testing at NASA Langley Research Center. *36th AIAA Aerospace Sciences Meeting and Exhibit*. 36th AIAA Aerospace Sciences Meeting and Exhibit, Reno,NV,U.S.A. https://doi.org/10.2514/6.1998-713

DeLoach, R. (2000). *The Modern Design of Experiments: A Technical and Marketing Framework*. 10.

English, T. G. (2007). *Application of Experimental Design for Efficient Wind Tunnel Testing: The Tandem Wing MAV Case*.

Ignatyev, D. I., Khrabrov, A. N., Kortukova, A. I., Alieva, D. A., Sidoryuk, M. E., & Bazhenov, S. G. (2020). Interplay of unsteady aerodynamics and flight dynamics of transport aircraft in icing conditions. *Aerospace Science and Technology*, *104*. https://doi.org/10.1016/j.ast.2020.105914

Kraber, S. (2021, May 20). *Avoiding Over-Selection of Effects on the Half-Normal Plot*. Statease.Com. https://www.statease.com/blog/avoiding-over-selection-of-effects-on-the-half-normal-plot/

Landman, D., Simpson, J., Hall, B., & Sumner, T. (2002). Use of Designed Experiments in Wind Tunnel Testing of Performance Automobiles. *SAE International*, 10. https://doi.org/10.4271/2002-01-3313

Sun, Y., Zhang, Y., Zhou, Y., Zhang, H., Zeng, H., & Yang, K. (2021). Evaluating Impact Damage of Flat Composite Plate for Surrogate Bird-Strike Testing of Aeroengine Fan Blade. *Journal of Composites Science*, *5*(7), 171. https://doi.org/10.3390/jcs5070171

Tatlıer, M. S., & Baran, T. (2020). Structural and CFD analysis of an airfoil subjected to bird strike. *European Journal of Mechanics*, 9.